Scilight

Smart Chemical Engineering
https://www.sciltp.com/journals/sce

Article

Physics-Informed Neural Network for Solving Forward and Inverse Problems of Granular Flow in the Homogeneous Cooling State

Bing Wan [1], Bidan Zhao [1,2,*], Lijing Mu [3] and Junwu Wang [1,4,*]

[1] Beijing Key Laboratory of Process Fluid Filtration and Separation, College of Mechanical and Transportation Engineering, China University of Petroleum-Beijing, Beijing 102249, China
[2] State Key Laboratory of Heavy Oil Processing, China University of Petroleum-Beijing, Beijing 102249, China
[3] Key Laboratory of Special Equipment Safety and Energy-Saving, State Administration for Market Regulation, China Special Equipment Inspection & Research Institute, Beijing 100029, China
[4] State Key Laboratory of Deep Geothermal Resources, China University of Petroleum-Beijing, Beijing 102249, China
* Correspondence: bdzhao@cup.edu.cn (B.Z.); jwwang@cup.edu.cn (J.W)

How To Cite: Wan, B.; Zhao, B.; Mu, L.; et al. TPhysics-Informed Neural Network for Solving Forward and Inverse Problems of Granular Flow in the Homogeneous Cooling State. *Smart Chemical Engineering* **2025**, *1*(1), 6. https://doi.org/10.53941/sce.2025.100006

Received: 9 August 2025
Revised: 5 October 2025
Accepted: 20 October 2025
Published: 6 November 2025

Abstract: The advent of machine learning has prompted the emergence of innovative methodologies for predicting the hydrodynamics of granular flows. In this study, the physics-informed neural network (PINN) approach was employed to solve the forward and inverse problems of a simple granular flow with smooth particles in the homogeneous cooling state. The three techniques, which are the dimensionless granular temperature as the optimization of the loss functions, the normalized time information as the input layer, and adjusting local weights of sample points based on the physical characteristics, have been shown to significantly contribute to enhancing the precision of classical PINN in predicting the variation of granular temperature over time. The proposed method (developed PINN) has been validated for many different cases and the influence of numbers of sampled date in the solution process was also investigated.

Keywords: machine learning; PINN; granular flow; Ggoverning equations; loss function

1. Introduction

The granular flows are widely present in the nature and the industrial fields, including pharmaceutical engineering, food engineering and numerous other disciplines [1]. Despite the presence of certain parallels with gas and liquid systems, these systems are distinguished by their distinct and more intricate hydrodynamics, a consequence of the dissipative solid particle constituting the fundamental element [2, 3]. The computational simulation has been identified as a prevalent methodology for the details of granular flows. The continuum model is rooted on a hypothesis that the granular flow is analogous to the gas or liquid flow. Under this assumption, the solid particles are considered to be similar to the gas molecules, thus enabling the application of mass, momentum and pseudo-energy conservation equations for describing the hydrodynamics of granular flows [4]. Furthermore, the constitutive relations related to the complex interaction between particles can be closed by kinetic theory of granular flow (KTGF) [5]. The accuracy of continuum model is dependent on the constitutive relations, such as the solid stress tensor [6]. However, the calculation of KTGF encompasses numerous strict assumptions, including the two-body interactions and molecular chaos [7–9]. Focusing on the motion of the single particle, the Lagrange method such as discrete element method (DEM) has the capability to analyze the interaction between solid particles and obtain the motion and location of any particles in a granular flow [10, 11]. In addition to the aforementioned points, it should be stressed that the computational time is always long for both classical methods, so there is still much room for improvement in the efficiency of the methods [12].

The advent of machine learning [13, 14] has prompted the emergence of innovative methodologies for the description of the hydrodynamics of granular flows [15, 16]. Since the moment of its inception, considerable attention

has been directed towards the Physics-Informed Neural Network (PINN) [17–21], with the objective of achieving a balance between interpretability and solution precision. This flexible neural network has been demonstrated to possess the capacity to construct intricate maps that encompass both inputs and outputs. The loss function is associated not only with the data themselves, but also with the physical laws that underpin the studied system. These include the partial differential equations that control the parameter optimization of the neural network, and it is these equations that ensure that the parameters satisfy the physical laws. Its extensive utilisations in resolving both forward and inverse problems pertaining to gas flows have been well-documented. In particular, its capability of solving inverse problems, which is the finding of whole flow fields from the underlying governing equations and few input (experimental) data, is quite unique, and therefore, should have a bright future in the study of granular flow and gas-solid flow, provided relevant technical challenges can be reasonably solved.

In this work, we made a try to utilize the PINN framework [20] to solving the forward and inverse problems of granular flow with smooth particles in the homogeneous cooling state (HCS) [22,23]. The implementation of three techniques in the PINN, namely the dimensionless granular temperature as the variable in the loss functions, the normalization of the time information as the input layer, and adjusting local weights of sample points based on the physical characteristics have been developed. Then this work investigated (I) when the governing equation is closed, whether the precision of this developed PINN has been enhanced the predictive precision for granular temperature for different operation conditions or not; (II) when the governing equation is unclosed, whether this developed PINN has the ability to solve a series of inverse problems for granular flow in the HCS. The remainder of this work is organized as follows: in the Section 2, the specific framework of this study is introduced; in the Section 3, the differences and connections between the classical PINN and developed PINN are discussed; Section 4 presents the results of the developed PINN in solving forward and inverse problems and the exploration of influencing factors for granular flow in HCS; and finally the Section 5 provides a summary of this work.

2. Granular Flow with Smooth Particles in Homogeneous Cooling State

The granular flow in the homogeneous cooling state can be considered as a simple system, where solid particles are distributed uniformly in the three-dimensional periodic domains at the beginning and the particle velocity $\mathbf{c}$ satisfies the Maxwellian distribution:

$$f(\mathbf{c}) = n(\frac{1}{2\pi\theta})^{\frac{3}{2}} \exp(-\frac{\mathbf{c}^2}{2\theta}), \tag{1}$$

where the related average macroscopic velocity of the whole domain is zero, n is the number density, and the fluctuating energy of granular flow is defined as the granular temperature $\theta = \frac{1}{3n} < \mathbf{c}^2 >$, and the granular temperature at initial time is denoted as θ_0. As time progresses, the granular temperature decreases due to the inelastic collisions between solid particles, and for a while, particles' spatial distribution remains uniform in the domain. This state of granular flow is designated as the homogeneous cooling state (HCS). Consequently, the sole governing equation that can be applied is the granular temperature equation [24]:

$$\frac{d\theta}{dt} = A\theta^{\frac{3}{2}}, \tag{2}$$

where the parameter in the dissipative source term A can be deduced by the kinetic theory of granular flow:

$$A = \frac{8(e^2-1)\varepsilon_s g_0}{d_p\sqrt{\pi}}, \tag{3}$$

and the radial distribution function $g_0 = \frac{1-0.5\varepsilon_s}{(1-\varepsilon_s)^3}$, where the restitution coefficient e quantifies the dissipative particle-particle collisions, d_p is the particle diameter and ε_s is the solid concentration. It is possible to obtain the variation of granular temperature with time by integrating Equation (2) with the help of initial granular temperature θ_0:

$$\theta = \theta_0\left(1 - \frac{A\theta_0^{\frac{1}{2}}}{2}t + \frac{A\theta_0^{\frac{1}{2}}}{2}t_0\right)^{-2}. \tag{4}$$

If the starting time is $t_0 = 0$, this expression of granular temperature (4) can be rewritten as $\theta = \theta_0/(1+t/\tau_0)^2$, where $\tau_0 \equiv -\frac{2}{A\theta_0^{\frac{1}{2}}}$. As the inelastic collision between particles continues for a long time, the particle within the system are no longer distributed uniformly. Instead, particle clusters gradually form in the domain. This state is not HCS any more, and is not the focus of present work.

In the pursuit of utilizing physics-informed neural networks to directly solve the granular flow, above simplest

granular flow in the HCS is identified as the subject for study. First of all, when the governing equation is closed, the changing of granular temperature over time has the analytical solution. We will use this fact for investigating the solving ability of forward problem of this simplest granular flow system using PINN. Then no matter missing the initial granular temperature θ_0 or missing the parameter of dissipated source term A, or missing both of them, the corresponding governing equation is not completed. This problem is called as the inverse one. Then we make a try to solve a series of inverse problems with the help of some sample calibration data for the granular flow in HCS. The variables under consideration and the material properties of the particles in the basic case of the granular flow system are illustrated in Table 1. It is evident that the comparison to the analytic solution, Equation (4), provides a clear demonstration of the predicted accuracy of PINN.

Table 1. Physical properties and simulation parameters.

Variable	Value
Particle number N	5×10^4
Particle diameter d_p (m)	1×10^{-3}
Particle density ρ_s $(\mathrm{kg/m^3})$	1500
Solid concentration ε_s	0.1
Side length of simulation domain L (m)	0.064
Restitution coefficient e	0.95
Total calculating time (s)	5
Initial granular temperature θ_0 $(\mathrm{m^2/s^2})$	0.01

3. Physics-Informed Neural Network

Physics-informed neural network, the frame diagram of classical version for the granular flow in HCS is shown in Figure 1, is a method to predict or reconstruct the field hydrodynamics described by the partial differential governing equations, which has attracted lots of attention since it was proposed. As in the single phase flow system, the input layer of PINNs is temporal and spatial information, which directly determines the temporal and spatial resolution of all obtained hydrodynamic variables in the output layer. Each hydrodynamic variable is corresponding to a temporal and spatial point one by one. The hidden layers in the neural network dig out the complex mapping relations between the input layer and output layer. In this work, the granular flow in the HCS has been focused, the input layer only relates to the temporal information, and the output layer is the corresponding granular temperature. Since the full connected neural network is chosen, the relationships between different layers in the neural network can be expressed as follows:

$$\begin{aligned} &\mathbf{z}^0 = (t) \\ &\mathbf{z}^k = \sigma(\mathbf{W}^k \mathbf{z}^{k-1} + \mathbf{b}^k), \quad 1 \le k \le L-1 \\ &\mathbf{z}^k = \sigma_{out}(\mathbf{W}^k \mathbf{z}^{k-1} + \mathbf{b}^k), \quad k = L \end{aligned} \tag{5}$$

where the output layer is the predicted granular temperature, i.e., $\hat{\theta} = \mathbf{z}^L$, where the layer number of this neural network is L. The weight matrix and bias vector of the k^{th} layer is denoted as $\mathbf{W}^k$ and $\mathbf{b}^k$, and $\sigma(\cdot)$ is the nonlinear activation function and $tanh$ is selected as activation function between the input layer and the hidden layers, as well as within the hidden layers. In order to ensure each element in the output layer as the granular temperature at the different time, which is constantly greater than 0, the activation function between the last layer of the hidden layers and the output layer is set as $\sigma_{out}(\mathbf{x}) \equiv softplus = \ln(1 + e^{\mathbf{x}})$. Moreover, the neural network can be expressed as $layers = [1, 128, 128, 128, 128, 1]$, which means the width of each hidden layer of the neural network has a number of 128 neurons, and this neural network includes a total of 4 hidden layers. The 1 in the input layer and output layer represents separately that the input layer has only one variable t, and the output layer has only granular temperature θ.

The vital part of PINN is the automatic differentiation technology. Once the weight matrix, the bias vector and the activation function are defined, the temporal and spatial differentiation of hydrodynamic variables of flow system can be calculated by the chain derivative laws. That means differentiation of hydrodynamic variables are directly by the numerous parameters of the neural network. In the classical neural network, the solved parameters only need to guarantee that the predicted hydrodynamic variables approximate the true values, which is the final optimized goal expressed as the loss function. However, in PINN, the optimization goal of numerous parameters is not only related to the data error as mentioned above but also related to the error of the governing equations. Thus the optimization

goal L for the granular flow in HCS is composed by the loss function corresponding to the governing equation L_{ODE}, the loss function corresponding to the initial condition L_{IC} and the loss function expressed as the distinction between the predicted granular temperature and the true one L_{Data} at the sampled points:

$$L = L_{ODE} + L_{IC} + L_{Data}, \tag{6}$$

where each parts can be expressed as

$$L_{ODE} = \frac{1}{N_t}\sum_{i=1}^{N_t}\left|\left|\left(\frac{d\hat{\theta}}{dt} - A\hat{\theta}^{\frac{3}{2}}\right)(t_i)\right|\right|_2^2, \tag{7}$$

$$L_{IC} = \left|\left|\hat{\theta}(t_0) - \theta(t_0)\right|\right|^2, \tag{8}$$

$$L_{data} = \frac{1}{N_{Data}}\sum_{i=1}^{N_{Data}} ||\hat{\theta}_i - \theta(t_i)||_2^2, \tag{9}$$

where the predicted variable is denoted as $\hat{\cdot}$, thus the granular temperature is $\hat{\theta}$ and the true granular temperature is denoted as θ, N_t is the total number of predicted granular temperature, N_{Data} means the number of sampled points, thus $N_t >> N_{Data}$ and both of them is not correlated with each other.

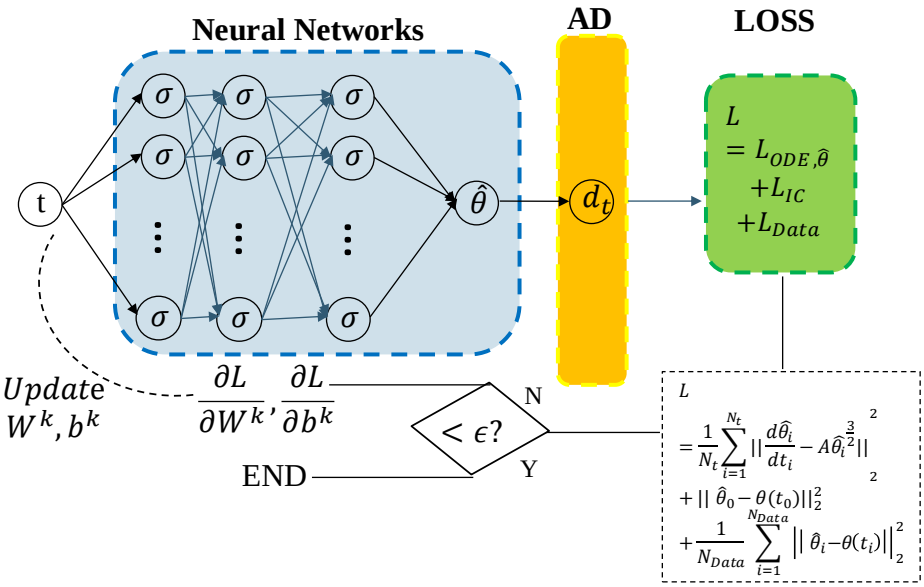

Figure 1. The frame diagram of classical PINN for the granular flow in HCS.

It is important to emphasise the following point: The investigation will explore the capabilities of PINN, when utilising two loss functions (L_{ODE} and L_{IC}), in addressing the temporal change in granular temperature. In this kind of forward problem, it is not necessary for the sample points to be included. In the case of the inverse problem, however, the inclusion of some sample points in the whole loss function is necessary in certain situations. These situations include the missing parameter of the dissipation source term for an incomplete governing equation, or missing the initial condition. In instances where the initial condition is absent, the loss functions associated with the complete governing equation and sampled points can be employed as the optimization objective for PINN. In certain instances, where both the uncompleted governing equation and missing initial condition are present, the objective of optimisation in PINN involves the utilisation of the uncompleted governing equation and the sampled points as the standard values.

Once the loss function is confirmed in PINN, substituting the results of the automatic differentiations about hydrodynamic variables into the loss function as the optimized goal, the classical parameter optimized algorithms such as Adam and L-BFGS-B, are utilised individually for the purpose of finding $\mathbf{W}^k$ and $\mathbf{b}^k$. The switching optimization algorithm is characterised by the Adam method, which is utilised for a limited number of iterations while the adapted learning rate is used. Subsequently, L-BFGS-B is employed for the purpose of parameter

optimization. In the event of the total loss function being very small and almost not changing at the point of Adam's termination, it is conceivable that L-BFGS-B will cease to be effective.

Considering the significant difference of the order of magnitude between the input layer $t \in [0, 5]$ and the output layer $\theta \in [10^{-5}, 10^{-2}]$, we make a try to establish developed PINN (as shown in Figure 2) with three following techniques for balancing the data difference. First of all, the time in the input layer can be normalized as follows:

$$\bar{t} = 2\frac{t - t_{min}}{t_{max} - t_{min}} - 1, \tag{10}$$

then, the value range of data in the input layer holds in $[-1, 1]$. Secondly, during the solution process, the dimensionless granular temperature is defined as $\bar{\theta} = \frac{\theta}{\theta_0}$. With the combination of the normalized time $\bar{t}$, the corresponding governing equation of granular temperature in the loss function of PINN can be rewritten as:

$$\frac{2}{t_{max} - t_{min}}\frac{d\bar{\theta}}{d\bar{t}} = A\theta_0^{\frac{1}{2}}\bar{\theta}^{\frac{3}{2}}. \tag{11}$$

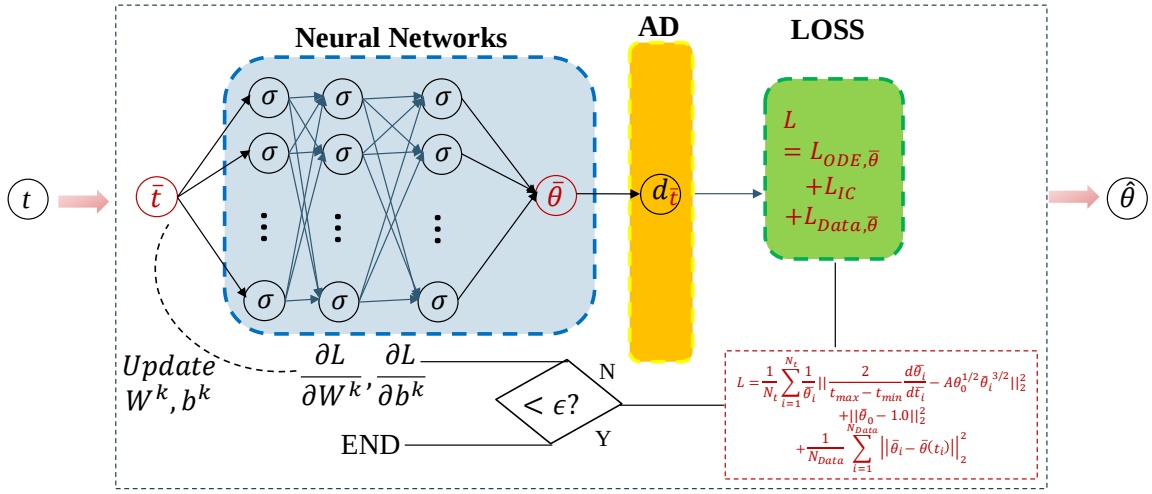

Figure 2. The frame diagram of developed PINN for the granular flow in HCS.

The combination of the normalized time as Equations (10) and (11) related to dimensionless granular temperature $\bar{\theta}$, ensures that the orders of magnitude of the input layer and output layer remain within the range of $[-1, 1]$. But in term of the changing rule of granular temperature over time, although the granular temperature has been dimensionless, there still are a significant difference between granular temperature at different moments. As time goes on, the contribution of the subsequent moment granular temperature governing equation to the whole loss function becomes smaller. This situation will result in the whole loss function based on Equation (11) being unable to constrain the governing equation to remain satisfied when the granular temperature being smaller. Therefore, we adjust the form of the loss function corresponding to the governing equation for balance the contribution of loss function corresponding to the granular temperature related to ODE as follows: by dynamically adjusting the local weight of the governing equation as $\frac{1}{\bar{\theta}_i}$, when the granular temperature is low, the corresponding governing equation weight in the whole loss function is large:

$$L_{ODE} = \frac{1}{N_t}\sum_{i=1}^{N_t}\frac{1}{\bar{\theta}_i}||\frac{2}{t_{max} - t_{min}}\frac{d\bar{\theta}_i}{d\bar{t}_i} - A\theta_0^{\frac{1}{2}}\bar{\theta}_i^{\frac{3}{2}}||_2^2. \tag{12}$$

It will be demonstrated that those optimized techniques facilitate the mapping between the normalized $\bar{t}$ and the dimensionless $\bar{\theta}$ more efficiently by PINN. Because of the two linear map relationships about one between $\bar{t}$ and t and another one between $\bar{\theta}$ and $\hat{\theta}$ are explicit, thus the developed-PINN have the capability to establish the map between t and $\hat{\theta}$. In other words, the developed-PINN has the capacity to predict the variation of granular temperature with time.

In addition to the above, we use sparse moments as input for PINN to verify its learning ability and verify its generalisation ability in denser temporal series as Figure 3. The time interval between sparse moments is 0.01, and the interval between dense data is 0.005.

In the following section, the application of developed PINN will be examined for the purpose of solving the forward and inverse problem of the granular flows in HCS. Meanwhile, the impact of the number of sample points on the predicted results of inverse problem has also been investigated.

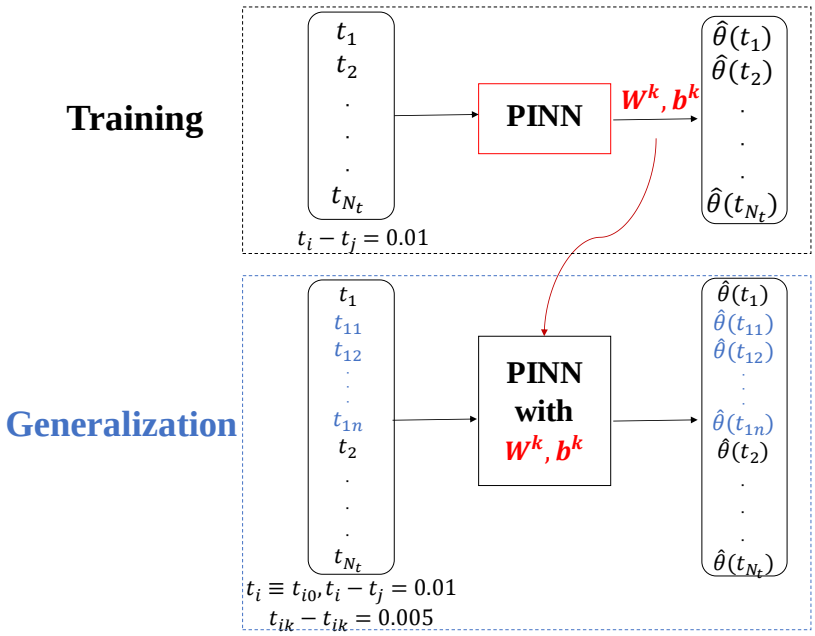

Figure 3. Training and generalization of classical/develoed PINN.

4. Result and Discussion

4.1. Forward Problem

First of all, we need to validate the developed PINN for solving the granular flow in the HCS and to demonstrate these three improvements included in PINN for improving the solving accuracy. As mentioned above, when the governing equation, constitutive relation such as dissipation source term, and the initial condition are complete, the variation of granular flow with time can be expressed by the analytical form. Thus we can compare the predicted results by classical and developed PINN with the analytical ones. At the aim of investigating the validation of PINN generally, here we focus on different cases besides basic case (Case1) as shown in Table 2.

Table 2. Different physical properties and simulation parameters in different cases.

Case Number	Different Physical Properties	Value	Time Interval [a]	Niter [b]	ILR [c]
1	Basic case as shown in Table 1	/	[0,5]	5×10^4	1×10^{-3}
2	Solid concentration ε_s	0.2	[0,5]	5×10^4	1×10^{-4}
3	Restitutive coefficient e	0.7	[0,1]	5×10^4	1×10^{-4}
4	Initial granular temperature T (m^2/s^2)	0.05	[0,5]	4.5×10^4	1×10^{-3}
5	Particle number N	1×10^5	[0,5]	5×10^4	1×10^{-3}
6	Particle diameter d_p (m)	2×10^{-3}	[0,5]	5×10^4	1×10^{-3}

[a] The unit is second; [b] Niter: Iterative number; [b] ILR: Initial learning rate of Adam.

In order to more effectively demonstrated the discrepancy in prediction, a relative error between the predicted value and the analytical value is defined as follows:

$$R(t_i) = \frac{|\theta_{predicted}(t_i) - \theta_{true}(t_i)|}{\theta_{true}(t_i)}, \tag{13}$$

and its mean is

$$\overline{R(t_i)} = \frac{1}{N_t} \sum_{i=1}^{N_t} R(t_i). \tag{14}$$

For these different cases, the classical PINN and the developed one have been utilized for solving the governing Equation (2). The corresponding results regarding the variation of granular temperature with time are shown in Figure 4. It can be seen that in comparison with the analytical solution, in a very short period of time, there is a substantial discrepancy in the granular temperature has been observed in the results obtained by the classical PINN. However, the developed PINN demonstrates a high level of accuracy in its predictions, with a satisfactory control error performance within the predicted time frame. Further, the mean relative error $\overline{R(t_i)}$ of developed PINN always are smaller than classical one as 2–4 magnitude within the predicted period as Figure 5.

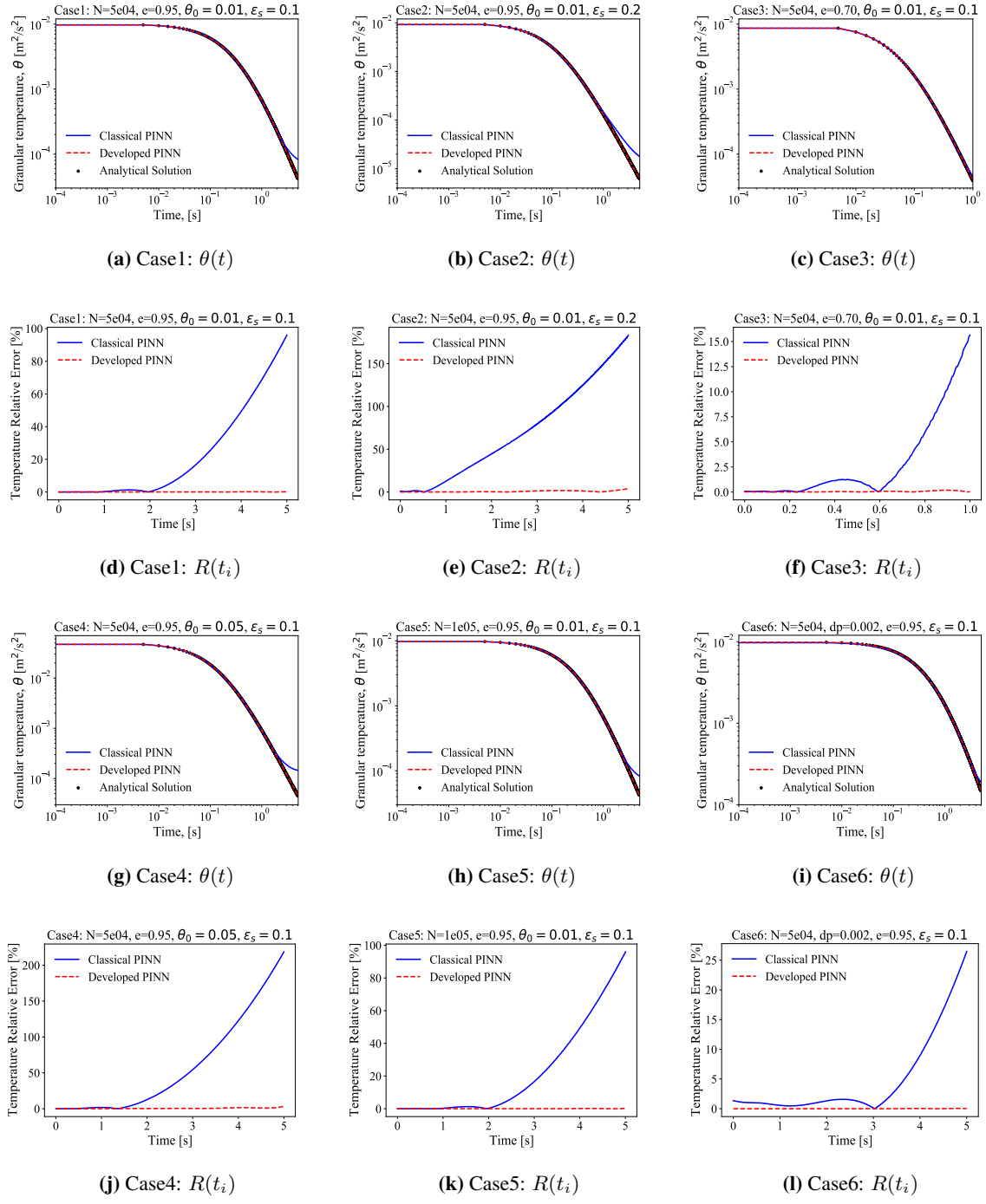

(a) Case1: $\theta(t)$ **(b)** Case2: $\theta(t)$ **(c)** Case3: $\theta(t)$

(d) Case1: $R(t_i)$ **(e)** Case2: $R(t_i)$ **(f)** Case3: $R(t_i)$

(g) Case4: $\theta(t)$ **(h)** Case5: $\theta(t)$ **(i)** Case6: $\theta(t)$

(j) Case4: $R(t_i)$ **(k)** Case5: $R(t_i)$ **(l)** Case6: $R(t_i)$

Figure 4. The predicted variation of granular temperature and relative error with time by PINNs compared by analytical solution as Equation (4).

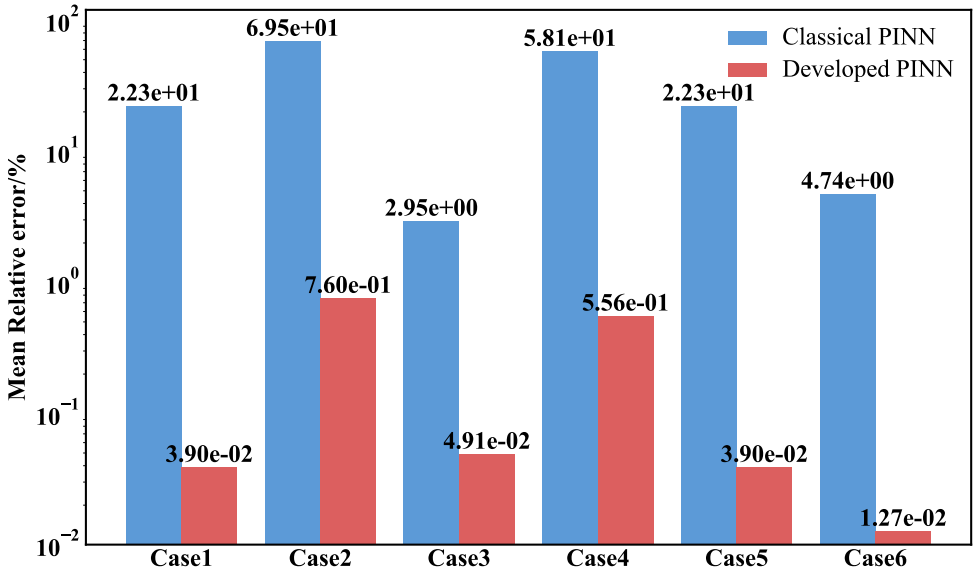

Figure 5. The comparsion of classical/develpoed PINN about the mean relative error of $\theta(t_i)$.

We further analyse the reasons for the differences in the predictive performance of two PINNs: normalized time and dimensionless granular temperature in developed PINN can keep the absolute value of both the input and output layer values around 1. Neural network make it relatively easy to find relationships between variables on the same order of magnitude. Overall. it appears that two techniques help to improve the predictive accuracy of developed PINN. However, the classical PINN predicted granular temperatures that differed significantly from the analytical solutions when the granular temperature becomes low. The novel developed PINN successfully managed to control the deviation by establishing dynamic local weights that were consistent with the physical characteristics. This resulted in larger weights being assigned to the governing equations at lower granular temperatures. This adjustment resulted in corresponding loss functions accounting for a greater proportion of the overall loss function, thereby necessitating compliance with this constraint. Consequently, the developed PINN demonstrated higher prediction accuracy when the granular temperatures were low.

The results presented in Figure 6 encompass both the training process and the generalization process of PINN. In the following, an analysis will be conducted of the training errors of the two PINN methods under conditions of small sizes of input layer, and of the generalization errors within the global temporal information as input layer. The investigation revealed that the training errors and generalization errors of the two methods are consistent, with both being similar to the global averaged relative error as Figure 5. It has been demonstrated that the PINN method exhibits favourable generalization performance for interpolation problems of granular flow in the HCS, as evidenced by the more precise moments in input layer obtained through the compression of the original sparse input layer. Besides, it has been demonstrated that, in both the training process and the generalization process, the accuracy of classical PINN is lower than that of developed PINN. This finding indicates that the incorporation of normalized time, dimensionless granular temperature, and dynamic local weights can effectively reduce the training and generalization errors of the PINN method when applied to granular flow.

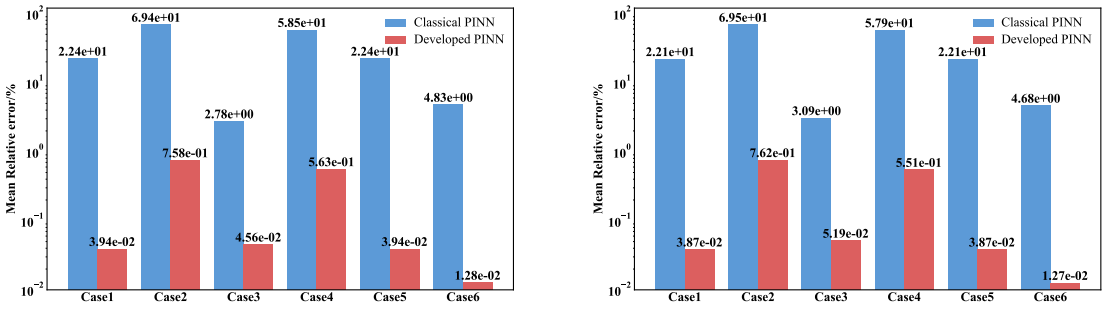

Figure 6. The mean relative error of classical/developed PINN in the training process and the generalization process. (**a**) The mean relative error in the training process; (**b**) The mean relative error in the generalization process.

We have proven the ability of the developed PINN to solve the forward problems of granular flow system in the HCS. Therefore, upon completion of the governing equation, constitutive relationships and initial/boundary value conditions, PINN can be utilized as a novel approach to substitute for conventional CFD solvers in the solution of granular flow systems.

In addition, for the complex granular flow systems, common modeling approach such as kinetic theory always make numerous assumptions, but we can obtain some measure data through experiments. Additionally, for the real industrial granular flow system, initial and boundary conditions are often difficult to determine. The system with the incomplete governing equation and initial/boudary conditions is referred to as an inverse problem, which is difficult to solve by traditional CFD or DEM methods. In the following part, our goal is to combine a small amount of experiment data with the developed PINN with the high precision to solve inverse problems in granular flow system.

4.2. Inverse Problem

Because of the validation of developed PINN being conducting for forward problems of many cases as mentioned above, furthermore, the granular temperature changes similarly over time. Nextly, for dealing with the inverse problems, only basic case (Case1) has been focused on. In the complete Case1, the initial granular temperature is $\theta_0 = 0.01$. We can use kinetic theory of granular flow to obtain A as Equation (3), and the variation of granular temperature over time can be calculated analytically and accurately by Equation (4). These can all be used as comparison values for solving inverse problems with the developed PINN. Specially, the inverse problems can be classified into three categories: The first category is characterized by an incomplete governing equation with a missing parameter A in the dissipation source term. The second category is characterized by a missing initial granular temperature θ_0. The third category is characterized by a missing parameter in the dissipation source term and the initial granular temperature. In the following, we will investigate the validation of the developed PINN for each inverse problem.

4.2.1. The First Inverse Problem: Missing the Parameter A in the Dissipation Source Term

For this kind of inverse problem, the form of loss function is the same as the Equation (6), which contains the first part L_{ODE} related to the incomplete governing ordinary differential equation with missing A, the second part L_{IC} related to the initial granular temperature and the third part L_{Data} related to the true granular temperature at same sampled time. At the same time, both of dimensionless granular temperature and normalized time have been substituted into the whole loss function, and the adjustment of local weights upon the governing equations with different times has been used to balance the contributions to the L_{ODE}. Thus, the whole loss function can be expressed as:

$$\begin{aligned} L =& L_{ODE} + L_{IC} + L_{Data} \\ =& \frac{1}{N_t}\sum_{i=1}^{N_t}\frac{1}{\bar{\theta}_i}||\frac{2}{t_{max}-t_{min}}\frac{d\bar{\theta}_i}{d\bar{t}_i} - A\theta_0^{\frac{1}{2}}\bar{\theta}_i^{\frac{3}{2}}||_2^2 + ||\bar{\theta}_0 - 1.0||_2^2 + \frac{1}{N_{Data}}\sum_{i=1}^{N_{Data}}||\bar{\theta}_i - \bar{\theta}(t_i)||_2^2 \end{aligned} \tag{15}$$

And in developed PINN, the initial learning rate of Adam is 1×10^{-4} and Adam iteration is 5×10^4. The number of sampled data in L_{Data} is 21.

The mean relative error of granular temperatures at sparse 501 moments learned by the developed PINN is 0.0433%. Then trained developed PINN has been used to predict for the granular temperature at other 500 moments, and the corresponding relative error is 0.0437%. Then whole predicted granular temperature at 1001 moments and the ensemble relative error within 0 to 5 s by the developed PINN is shown in the Figure 7, where the mean relative error is 0.0435%. For this first inverse problem, the developed PINN demonstrates comparable training and generalization performance, while exhibiting high accuracy in the representation of granular temperature variations over time.

By comparing with results for the forward problem of Case1, the ensemble mean relative error is only 0.0045% higher than the one related to forward problem. On one side, this result is still encouraging, because traditional methods such as CFD cannot solved this problems such as the granular flow without the complete governing equations. On the other hand, this indicates that incorporating complete governing equations into the loss function helps to improve the accuracy of PINN predictions of granular temperature of the granular flow in the HCS.

In this kind of inverse problem, in addition to the granular temperature, the parameter of dissipation source term A need to be learned out. Here, with the combination of the 500 temporal points in input layer, the developed PINN has predicted to value of A as $A = -57.3452$, the corresponding relative error is 0.0044% by comparing with the analytical result by KTGF. These results indicate that the developed PINN has the capacity to address not only

the hydrodynamics of granular flow systems but also the constitutive relationships that are challenging to determine in the governing equations. As mentioned in the introduction, the classical methods such as KTGF or DEM statistical method for determining solid phase constitutive relationships are all subject to certain limitations. Thus, this approach is instrumental in establishing the constitutive relationships for the complex granular flow systems.

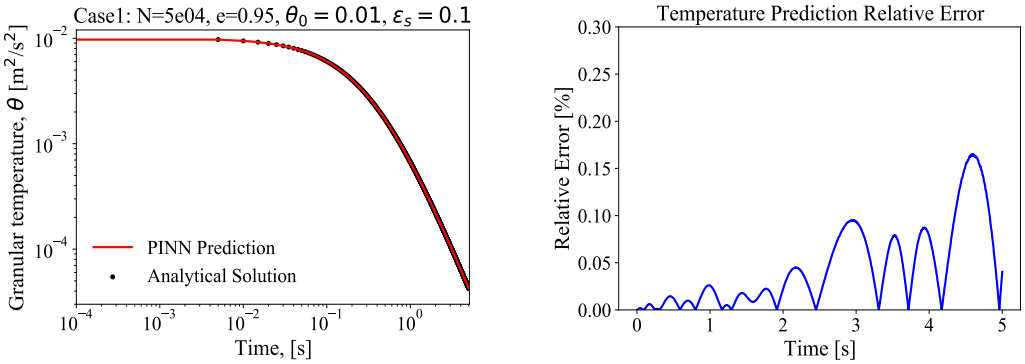

(a) Case1: $\theta(t)$ **(b)** Case1: $R(t_i)$

Figure 7. In the first inverse problem, the predicted variation of granular temperature and relative error with time by developed PINNs compared by the analytical solution as Equation (4).

4.2.2. The Second Inverse Problem: Missing the Initial Granular Temperature θ_0

The second inverse problem of granular flow in HCS is only missing the initial granular temperature. This problem also can not be solved by the classical method. We have made a try to solve this problem by the developed PINN, and the related ensemble loss function without L_{IC} is as follows and the parameter A is determined by KTGF:

$$\begin{aligned} L =& L_{ODE} + L_{Data} \\ =& \frac{1}{N_t}\sum_{i=1}^{N_t}\frac{1}{\hat{\theta}_i}||\frac{2}{t_{max}-t_{min}}\frac{d\hat{\theta}_i}{d\bar{t}_i} - A\hat{\theta}_i^{\frac{3}{2}}||_2^2 + \frac{1}{N_{Data}}\sum_{i=1}^{N_{Data}}||\hat{\theta}_i - \theta(t_i)||_2^2 \end{aligned} \tag{16}$$

It's worth to stressing that: since the initial granular temperature is missing from this inverse problem, it is impossible to perform dimensionless granular temperature. Therefore, all granular temperatures involved in the developed PINN of this part have dimensions. The other two techniques-normalized time and dynamic adjustment of local weights-are also incorporated. Through these techniques in the developed PINN, we hope to learn the time-dependent relationship of granular temperature and the initial granular temperature in this inverse problem. In the specific calculation, initial learning rate, iteration number of Adam and number of sampled date hold the same as the first inverse problem.

The specific learning results are as follows: for this inverse problem, PINN demonstrates its capacity to identify the temporal decay pattern of granular temperature as shown in Figure 8a. Additionally, it exhibits a substantial reduction in the relative error associated with predicting the temporal variation of granular temperature in Figure 8b. This finding suggests that the utilization of dimensioned granular temperature, in conjunction with the dynamic adjustment of local weights, enhances the accuracy of predictions for smaller granular temperatures. The substantial initial granular temperature error is attributable to the absence of initial granular temperature constraints. The mean relative error of granular temperature is 0.1061% for 1001 moments, and predicted initial granular temperature is 0.009971, the corresponding relative error about it is 0.2865%. A comparison of these error with those of the forward problem reveals an increase in both, thereby confirming the hypothesis that incomplete constraints indeed reduce the solution accuracy of developed PINN. Concurrently, it is critical to accurately determine the initial operation condition of the granular flow system. This is due to the fact that, in industrial granular flow systems, it is challenging to precisely ascertain the initial operation condition. However, it is critical to the subsequent evolution of the flow field.

4.2.3. The Third Inverse Problem: Missing Both of A and θ_0

For the third inverse problem of missing A and θ_0, the ensemble loss function is set as the same form as Equation (17) firstly, where the parameter A of dissipation source term in the governing equation retains to miss. In this problem, both of the missing initial granular temperature θ_0 and the parameter of dissipation source term A are treated as unknown parameters and participate in the iterative optimization of the entire network. Within the

framework of this specific learning process, the learning rate is maintained at 0.001, while the number of sampling points remains constant 21. However, the total number of optimizing iterations is increased to 2×10^5.

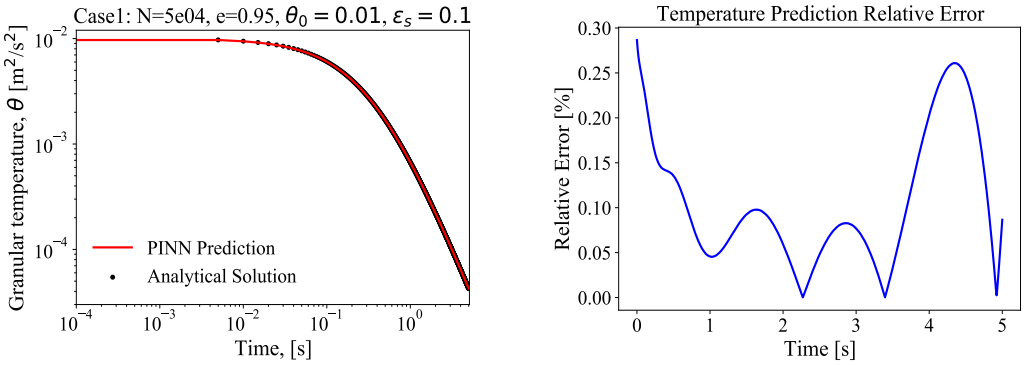

(a) Case1: $\theta(t)$ **(b)** Case1: $R(t_i)$

Figure 8. In the second inverse problem, the predicted variation of granular temperature and relative error with time by developed PINNs compared by analytical solution as Equation (4).

As demonstrated by the Figure 9, in the third type of inverse problem, where both A and θ_0 are missing, if the global weights of each part of the loss function are maintained as being equal with each other ($Weight_{ODE} = 1$, $Weight_{Data} = 1$), the granular temperature predicted by PINN during training and generalization exhibits significant deviation from the analytical solution over time. The mean relative error can reach 149.56% (Figure (10)), and when the granular temperature decreases its minimum, the maximum relative error can reach approximately 200%. It is hypothesised that this may be attributable to the fact that this inverse problem involves incomplete governing equation and initial conditions, resulting in overly relaxed constraints on these two components. It is evident that this hinders the capacity of the overall loss function to accurately constrain parameter optimization, consequently resulting in erroneous outcomes being obtained from the network. However, it is important to note that the constraints imposed on the loss function at the data calibration points are both correct and complete. The central question guiding this study is whether an increase in the global weights of this part of the loss function would result in more accurate predictions of the overall granular temperature results. Then we rewrite the loss function with adjusting the global weight of developed PINN in the third inverse problem:

$$\begin{aligned} L =& L_{ODE} + L_{IC} + Weight_{Data} * L_{Data} \\ =& \frac{1}{N_t} \sum_{i=1}^{N_t} \frac{1}{\hat{\theta}_i} || \frac{2}{t_{max} - t_{min}} \frac{d\hat{\theta}_i}{d\bar{t}_i} - A\hat{\theta}_i^{\frac{3}{2}} ||_2^2 + Weight_{Data} * \frac{1}{N_{Data}} \sum_{i=1}^{N_{Data}} ||\hat{\theta}_i - \hat{\theta}(t_i)||_2^2 \end{aligned} \tag{17}$$

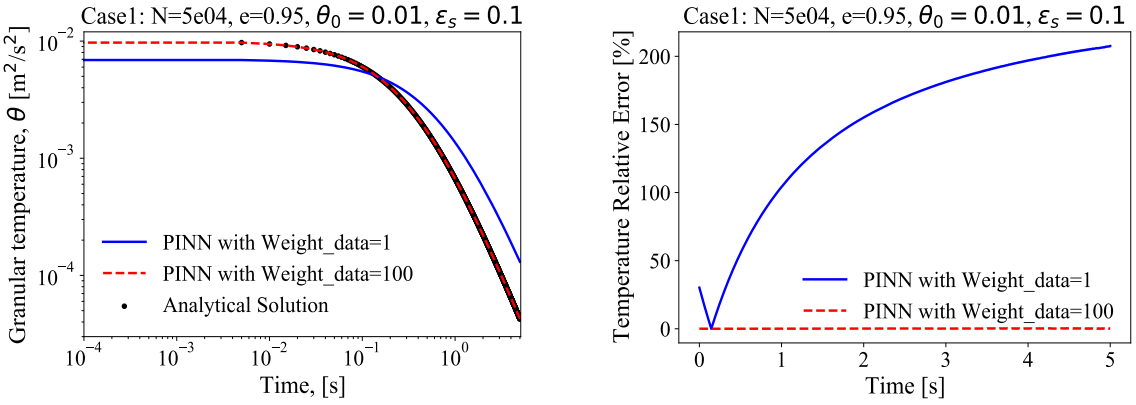

(a) Case1: $\theta(t)$ **(b)** Case1: $R(t_i)$

Figure 9. In the third inverse problem, the predicted variation of granular temperature and relative error with time by developed PINNs compared by analytical solution as Equation (4), where $Weight_{ODE} = 1, Weight_{IC} = 1$, $Weight_{Data} = 1$ or 100.

Subsequently, the above loss function with adjusting global weight $Weight_{Data}$ of L_{Data}, is integrated into the developed PINN framework. This investigation continues to explore the relationship between the average relative error of granular temperature $\overline{R(t_i)}$ and $Weight_{Data}$. It has been demonstrated in Figure 10 that, upon increasing the weight from 1 to 50, the average relative error can be reduced from approximately 150% to approximately 1.7%. It is evident that increasing $Weight_{Data}$ to 100 can effectively regulate the average relative error to 0.187%, thereby ensuring its maintenance below 1%. Thus in the following, the global weights for the third inverse problem are set to $Weight_{ODE} = 1$, and $Weight_{Data} = 100$.

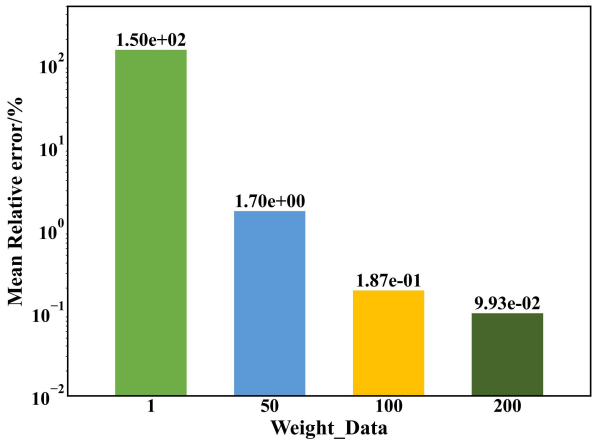

Figure 10. In the third inverse problem, the effect of $Weight_{Data}$ on the mean relative error of granular temperature.

When $Weight_{Data} = 100$, the developed PINN successfully predicts the missing parameter A and the initial granular temperature θ_0, with mean relative error 0.134% and 0.0719% by compared with analytical results from KTGF. The above results indicate that for granular flow systems with incomplete governing equations and initial conditions, the developed PINN has the potential to accurately determine hydrodynamics of the entire flow field based on a small number of the observed experimental sample points as shown in Figure 9, furthermore, at all times, the global overall error predicted by the developed PINN is controlled below 0.2%. However, in this process, it is necessary to strengthen the global weight $Weight_{Data}$ of the loss function L_{Data} related to data sample points. It also indicates that different global weight proportions of each part of the PINN loss function ($Weight_{ODE}$, $Weight_{IC}$, $Weight_{Data}$) will have a significant impact on the predicted results.

4.2.4. The Effect of the Number of Sample Data N_{Data} on the Predicted Results by the Developed PINN

As shown in Figure 11, the qualitative effect of the sample size on the predicted results of the mean relative error of granular temperature is consistent for the three different inverse problems. As the sample size increases, the mean relative error of granular temperature first decreases and then increases. Specifically, when the sample size is only 2% ($N_{Data} = 11$, $11/501 \approx 2\%$), the mean relative error of granular temperature is largest. When the sample size increases to 4% ($N_{Data} = 21$, $21/501 \approx 4\%$), the mean relative error decreases. Further increasing the sample size to 10% ($N_{Data} = 51$, $51/501 \approx 10\%$) results in a slight decrease in the relative error. Finally, when the sample size increases to 20% ($N_{Data} = 101$, $101/500 \approx 20\%$), the relative error begins to increase slightly compared to that at 10%. As the sample size increases, the optimized loss function becomes more complex. Therefore, when selecting a sample size for an inverse problem of granular flow, a balance must be struck between computational accuracy and learning efficiency.

In above three inverse problems, it is important to make predictions not only for the temporal variation of granular temperature but also for the missing constitutive relationships and initial conditions. In order to select the number of calibrated sample points, it is also necessary to take the accurate prediction for these parameters into consideration. Some relevant results are presented as in Figure 12: In the first inverse problem, it is evident that as the quantity of sampled data points is increasing, the complexity of the loss function is increased, consequently resulting in a gradual diminution of the predictive capability of parameter A in the dissipation source term of the governing equation. This observation indicates that an excessive number of sample points may induce overfitting during parameter prediction optimization within the developed PINN. In the second and third inverse problems, the error in parameter prediction initially diminishes before increasing as the number of sampling calibration points increases. For second inverse problem, this change is not very noticeable, with the relative error in initial granular temperature remaining between 0.287% and 0.659%. The overall error is minimal for varying numbers of sampling points. The minimum parameter prediction error is achieved with 21 sampling points, accounting for 4% of the total training

data samples. This finding suggests that, in second inverse problem, where only the initial granular temperature is absent, the number of sampling calibration points has minimal influence on the parameter prediction results. However, for the third inverse problem, which is the inverse problem with the most missing information, when the total number of calibration sampling points is only 2% of the total data, the error in two-parameter prediction can reach the order of magnitude of 1%. It is evident that the increase of the number of sampling points results in a reduction of the overall parameter prediction error by one to two orders of magnitude. Concurrently, the minimal relative parameter error is observed at a data scale of approximately 4%. Further comparison of the prediction results for parameter A in the first/third inverse problems reveals that, under the same calibration data sample size, the first problem is simpler and therefore achieves higher accuracy in predicting parameter A. When we continue to comparing the prediction results for the initial granular temperature between the second/third inverse problems, we found that, although the second problem is simpler, the third problem achieves higher prediction accuracy for the initial granular temperature when the data volume increases within the range of 4% to 20%. However, when the data volume is small (2%), the developed PINN provides more accurate predictions of second inverse problem. This analysis shows that the number of sample calibration points should be selected based on the complexity of the problem and the underlying physical laws.

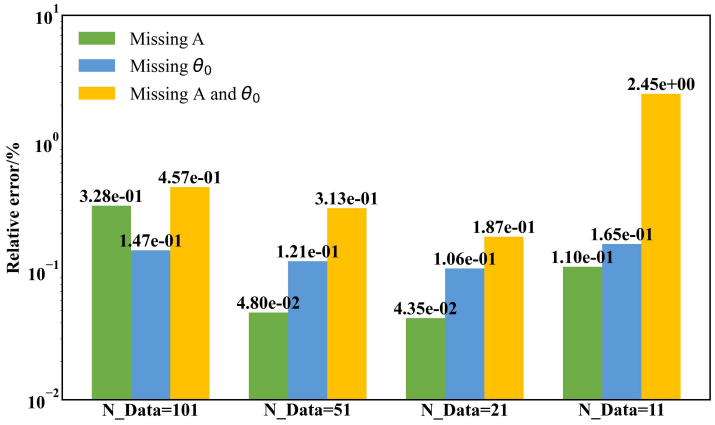

Figure 11. The effect of the number of sample data N_{Data} on the predicted granular temperature during the time period of interest by developed PINN in three different inverse problems.

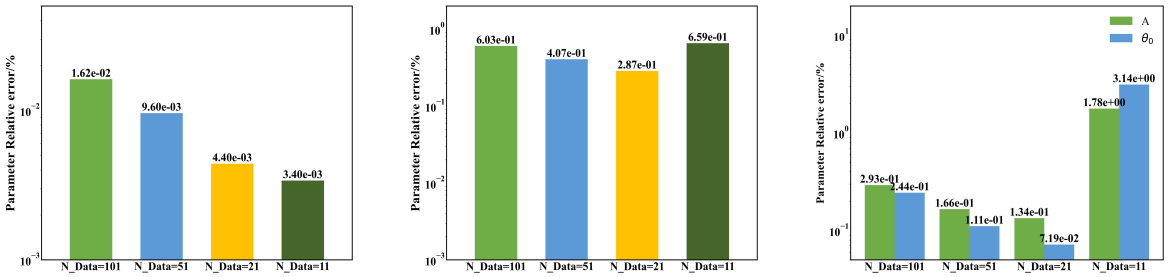

Figure 12. The effect of the number of sample data N_{Data} on the parameter A/ the initial granular temperature θ_0 by developed PINN in different inverse problem of granular flow in the HCS. (**a**) The parameter A of the first inverse problem; (**b**) The initial granular temperature θ_0 of the second inverse problem; (**c**) Both A and θ_0 of the third inverse problem.

5. Conclusions

This work has used the classical physics-informed neural network (PINN) for solving the governing equation with the initial condition as forward problem for the granular flow with smooth particles in the homogeneous cooling state. In order to enhance the precision of the specific solution, the developed PINN with dynamic local weight incorporates both of the normalized time as the input layer and the dimensionless granular temperature as the output layer. The developed PINN demonstrates the capacity to predict the change in the granular temperature over an extended time period with greater accuracy in comparison to the classical PINN. In addition, we employed a combination of developed PINN and a limited number of analytically calibrated sample points to address three

distinct types of inverse problems for granular flow: the absence of parameter A in the dissipation source term, the absence of initial granular temperature θ_0, and both the absent parameters A and θ_0. The findings demonstrate the application of PINN in accurately resolving these three types of inverse problems. The method not only can predict the change in granular temperature over time but also can predict the missing parameters. Further analysis indicates that, for the most complex inverse problem as the third one, it is necessary to increase the weight of the loss function for the observed sample points for increasing the accuracy of prediction. Meanwhile, the number of observed sample points has been demonstrated to exert a certain degree of influence on the final solution results, with the solution accuracy initially decreasing and subsequently increasing as the number of sample points increases. This work demonstrates the potential capabilities of PINNs in solving forward and inverse problems in granular flow systems. Concurrently, the aforementioned optimization techniques for PINN, in conjunction with the number of the sampling points and adjusted global weights that necessitate particular consideration, are of paramount importance for the future study of industrial complex granular flow systems.

Author Contributions

B.W.: Data curation (lead), Software (lead), Validation(Supporting); B.Z.: Conceptualization (lead), Data curation (supporting), Formal analysis (lead), Funding acquisition (lead), Investigation (lead), Methodology (lead), Project administration (lead), Resources (lead), Software (supporting), Supervision (lead), Validation (lead), Visualization (lead), Writing—original draft (lead), Writing—review & editing(lead); L.M.: Funding acquisition (supporting), Writing—review & editing(supporting); J.W.: Conceptualization (supporting), Formal analysis (supporting), Funding acquisition (supporting), Investigation (supporting), Methodology (supporting), Project administration (equal), Resources (supporting), Supervision (supporting), Validation (supporting), Writing—review & editing(supporting). All authors have read and agreed to the published version of the manuscript.

Funding

This study is financially supported by the National Natural Science Foundation of China (22378399, 22478421), the Young Elite Scientists Sponsorship Program by CAST (2022QNRC001), and the Science Foundation of China University of Petroleum (Beijing) (2462024YJRC012, 2462024YJRC008).

Data Availability Statement

These codes for classical PINN and developed PINN are available though Github at https://github.com/bdzhao-cup/PINN_for_granular_flowHCS.git.

Conflicts of Interest

The authors declare no conflict of interest.

Use of AI and AI-Assisted Technologies

No AI tools were utilized for this paper.

References

1. Rao, K.K.; Nott, P.R.; Sundaresan, S. *An Introduction to Granular Flow*; Cambridge University Press: Cambridge, UK, 2008.
2. Jaeger, H.M.; Nagel, S.R.; Behringer, R.P. Granular solids, liquids, and gases. *Rev. Mod. Phys.* **1996**, *68*, 1259–1273.
3. Kadanoff, L.P. Built upon sand: Theoretical ideas inspired by granular flows. *Rev. Mod. Phys.* **1999**, *71*, 435–444.
4. Wang, J. Continuum theory for dense gas-solid flow: A state-of-the-art review. *Chem. Eng. Sci.* **2020**, *215*, 115428.
5. Gidaspow, D. Multiphase Flow and Fluidization: Continuum and Kinetic Theory Descriptions; *Academic Press*: San Diego, CA, USA, 1994.
6. Zhao, B.; Wang, J. Kinetic theory of polydisperse gas–solid flow: Navier–Stokes transport coefficients. *Phys. Fluids* **2021**, *33*, 103322.
7. Luding, S. On the relevance of molecular chaos for granular flows. *J. Appl. Math. Mech.* **2000**, *80*, 9–12.
8. Costantini, G.; Puglisi, A. Role of Molecular Chaos in Granular FluctuatingHydrodynamics. *Math. Model. Nat. Phenom.* **2011**, *6*, 2–18.
9. He, M.; Zhao, B.; Xu, J.; et al. Assessment of kinetic theory for gas–solid flows using discrete particle method. *Phys. Fluids* **2022**, *34*, 093315.
10. Cundall, P.A.; Strack, O.D. A discrete numerical model for granular assemblies. *Geotechnique* **1979**, *29*, 47–65.
11. Guo, Y.; Curtis, J.S. Discrete element method simulations for complex granular flows. *Annu. Rev. Fluid Mech.* **2015**, *47*, 21–46.

12. Zhang, S.; Ge, W.; Liu, C. Spatial–temporal multiscale discrete–continuum simulation of granular flow. *Phys. Fluids* **2023**, *35*, 053319.
13. Brunton, S.L.; Noack, B.R.; Koumoutsakos, P. Machine learning for fluid mechanics. *Annu. Rev. Fluid Mech.* **2020**, *52*, 477–508.
14. Zhu, L.T.; Chen, X.Z.; Ouyang, B.; et al. Review of Machine Learning for Hydrodynamics, Transport, and Reactions in Multiphase Flows and Reactors. *Ind. Eng. Chem. Res.* **2022**, *61*, 9901–9949.
15. Guan, S.; Qu, T.; Feng, Y.; et al. A machine learning-based multi-scale computational framework for granular materials. *Acta Geotech.* **2023**, *18*, 1699–1720.
16. Cheng, C.H.; Lin, C.C. Prediction of force chains for dense granular flows using machine learning approach. *Phys. Fluids* **2024**, *36*, 083306.
17. Raissi, M.; Perdikaris, P.; Karniadakis, G.E. Physics-informed neural networks: A deep learning framework for solving forward and inverse problems involving nonlinear partial differential equations. *J. Comput. Phys.* **2019**, *378*, 686–707.
18. Raissi, M.; Yazdani, A.; Karniadakis, G.E. Hidden fluid mechanics: Learning velocity and pressure fields from flow visualizations. *Science* **2020**, *367*, 1026–1030.
19. Karniadakis, G.E.; Kevrekidis, I.G.; Lu, L.; et al. Physics-informed machine learning. *Nat. Rev. Phys.* **2021**, *3*, 422–440.
20. Cai, S.; Mao, Z.; Wang, Z.; et al. Physics-informed neural networks (PINNs) for fluid mechanics: A review. *Acta Mech. Sin.* **2021**, *37*, 1727–1738.
21. Jin, X.; Cai, S.; Li, H.; et al. NSFnets (Navier-Stokes flow nets): Physics-informed neural networks for the incompressible Navier-Stokes equations. *J. Comput. Phys.* **2021**, *426*, 109951.
22. Brito, R.; Ernst, M. Extension of Haff's cooling law in granular flows. *Europhys. Lett.* **1998**, *43*, 497.
23. Miller, S.; Luding, S. Cluster growth in two-and three-dimensional granular gases. *Phys. Rev. E* **2004**, *69*, 031305.
24. Zhao, B.; He, M.; Wang, J. Data-driven discovery of the governing equation of granular flow in the homogeneous cooling state using sparse regression. *Phys. Fluids* **2023**, *35*, 013315.